ISBN: 978-3-95450-201-1 doi:10.18429/JACoW-IBIC2018-TUOB03

DEMONSTRATION OF A NEWLY DEVELOPED PULSE-BY-PULSE X-RAY BEAM POSITION MONITOR IN SPring-8*

Hideki Aoyagi†, Yukito Furukawa, Sunao Takahashi, Atsuo Watanabe
Japan Synchrotron Radiation Research Institute (JASRI), Hyogo, Japan

Abstract

A newly designed pulse-by-pulse X-ray beam position monitor (XBPM), which is photoemission type, has been demonstrated successfully in the SPring-8 synchrotron radiation beamline. Conventional XBPMs work in the direct current (DC) mode, because it is difficult to measure a beam position in the pulse mode under the severe heat load condition. The key point of the design is aiming at improving heat-resistance property without degradation of high frequency property. This monitor is equipped with microstripline structure for signal transmission line to achieve pulse-by-pulse beam position signal. A photocathode is titanium electrode that is sputtered on a diamond heat sink to achieve high heat resistance. We have manufactured the prototype, and demonstrated feasibility at the SPring-8 bending magnet beamline. As a result, we observed a unipolar single pulse with the pulse length of less than 1 ns FWHM and confirmed that it has pulse-by-pules position sensitivity. Furthermore, this monitor can be also used in the DC mode with good stability and good resolution. The operational experience will be also presented.

INTRODUCTION

Development of a pulse-by-pulse X-ray beam position monitor (XBPM) aiming at measuring every isolated pulses for insertion devise (ID) beamline of the synchrotron radiation facility SPring-8 is being advanced. Conventional XBPMs used widely are photoemission type, and blade-shaped tungsten is usually employed as a detector head to raise heat-resistance [1]. However, it is impossible to measure the beam position of every isolated pulses with the conventional XBPMs, because of long time constant of the current signal and ringing due to stray capacitance and impedance mismatch. Therefore, we tried to settle this problem by adopting polycrystalline diamond as a heat sink to improve the heat resistance, and downsized detector heads to reduce the stray capacitance [2]. In addition, the microstripline structure [3-6] is adopted in the vacuum chamber of the monitor to prevent attenuation and reflection of the unipolar single pulse.

DESIGN AND MANUFCTURE

The pulse-by-pulse XBPM that we have been developing is photoemission type in the same way as the conventional XBPMs, and having four blade-shaped diamond heat sinks with titanium plated electrodes (detector heads) in top/bottom and right/left near the beam axes to measure the beam position in horizontal and vertical directions. The detector heads are inclined by 1/20 against the beam axis to be irradiated mainly on the unilateral side of the blade. As a result, photoemission can be controlled efficiently with the applied voltage of the charge collecting electrodes (collectors).

Figure 1 (a) shows a photograph of diamond heatsinks mounted on the water-cooling base. According to the thermal finite element analysis [7, 8], the thermal contact conductance between the heat sink and the cooling holder needs to be $>10^4$ W/(m^2·K). Therefore, indium foils of the 50μm thickness are inserted between them to improve the thermal contact conductance. Figure 1 (b) shows a photograph of a signal transmission line with microstripline structure, which is mounted on an ICF70 flange. According to the high frequency properties test, the time domain reflectometry using the pilot model of the detector head has been performed in advance. It was confirmed that the unipolar single pulse of sub-nanosecond can be obtained [7, 8].

Figure 2 shows a 3D image of the combination of the detector head (Fig. 1 (a)) and the microstripline structure (Fig. 1 (b)). The structure of the pulse-by-pulse XBPM is shown in Fig. 3. The shading mask is mounted directly on the upstream side of the 6-way cross-chamber to prevent the cooling base from irradiation. By arranging a pair of collectors on both sides of left and right of the detector heads, photoelectron emitted from the detector heads can be attracted or retarded according to the polarity of the collector. In the direct current (DC) mode operation, in the same way as the conventional XBPM, current signal can be stabilized by applying the voltage, which is usually +100 V. In the pulse-mode operation, the negative voltage is applied to retard the emission of low energy photoelectron that distort the pulse waveform.

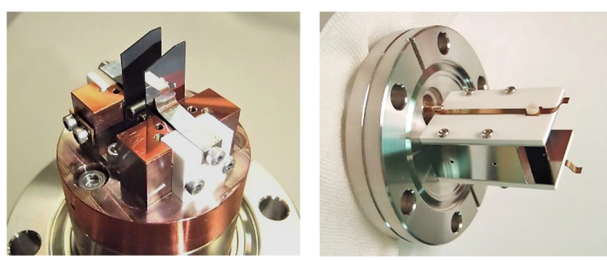

(a) (b)

Figure 1: (a) Photograph of diamond heatsinks (20 mm × 8 mm × 0.3 mm). (b) Photograph of signal transmission lines with microstripline structure.

* This work was partly supported by Japan Society for the Promotion of Science through a Grant-in-Aid for Scientific Research (c), No. 20416374 and No. 18K11943.
† aoyagi@spring8.or.jp

ISBN: 978-3-95450-201-1 doi:10.18429/JACoW-IBIC2018-TUOB03

This monitor was installed in the SPring-8 bending magnet beamline BL02B1 frontend and performance tests have been carried out [9]. Among four signal cables, HUBER+SUHNER, SucoFeed 1/2", which has small attenuation, is used for one of the cables (UL, upper-left) to observe a pulse waveform. As for the three remaining cables, HUBER+SUHNER, S-04272B is used because the DC mode measurement is mainly performed.

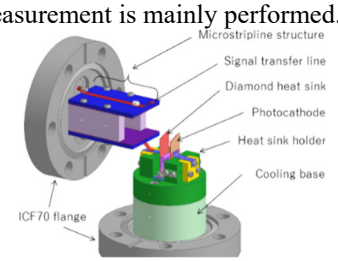

Figure 2: Combination of detector heads and microstripline structure.

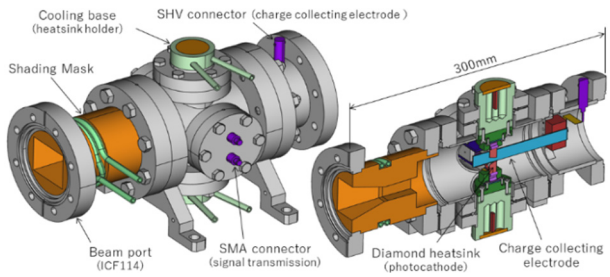

Figure 3: Structure of a monitor chamber.

PERFORMANCE IN PULSE-MODE

Observation of the Pulse Waveform

Figure 4 shows the typical pulse waveform of the current signal of this monitor. The filling pattern of the storage ring was "1/7 filling + 5 bunches" mode, and the isolated unipolar single pulse is observed. Oscilloscope is used for pulse waveform observation under the conditions of 4 GHz B. W., 20 GS/s, 100-time average. The pulse length with a full width at half maximum (FWHM) of 0.8 ns was obtained. As shown in Fig. 5, the various pulse waveforms were observed by changing the voltage of the collectors. The pulse waveform (height, length) greatly depends on polarity and height of the voltage. It can be seen that lowering the applied voltage decreases the pulse height and width. However, as the negative voltage is increased, the double peak at the top of the pulse waveform becomes obvious. The reason for this phenomenon cannot be explained by the resonance of the high frequency component in the vacuum vessel, because it would decays over time if it is a resonance. For the same reason it is not a reflection between the blade tip and the end of the microstripline structure. We can understand the cause of the double peak in the following way. The first peak is caused by photoelectrons reaching the collector with high energy enough not to be affected by the voltage of the collector. In addition, the second peak occurs because low-energy photoelectrons reach the collector with a little delay while being decelerated by the negative voltage of the collector.

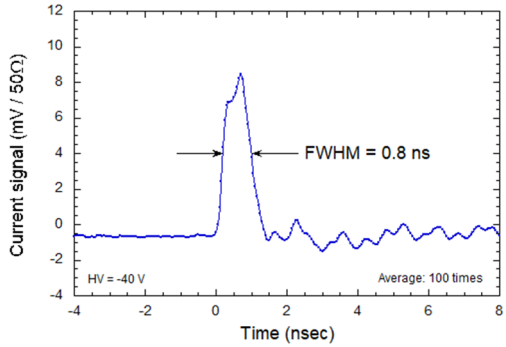

Figure 4: Pulse waveform of current signal.

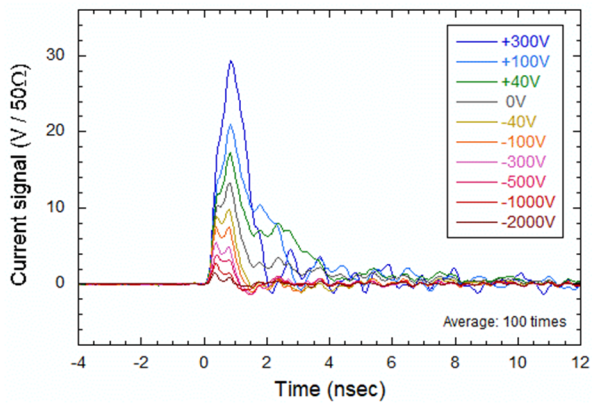

Figure 5: Various waveforms due to difference in applied voltage.

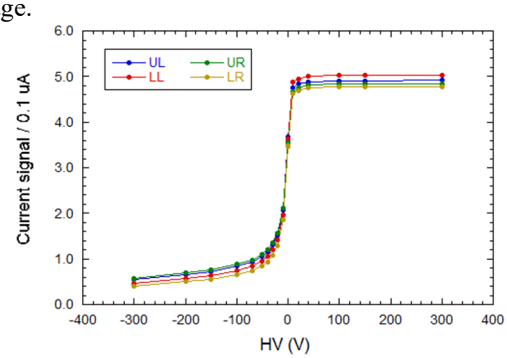

Figure 6: Applied voltage dependence of current signal.

Figure 6 shows the current signal with respect to the applied voltage of the collector using this monitor in the DC mode same as the conventional monitor. The current signal of each blade is greatly changed, especially around 0 V of the collector, and the retarding effect is obvious on the negative side. The reason for this is that the blades of this monitor have a slight inclination from parallel to the beam axis and only one side of the outside of the blades are irradiated so that the effective electric field is high. As a result, it is possible to suppress emission of slow electrons of several tens of volts, and to suppress increase in pulse length. When the voltage of the collector is +40 V or more, the current signal keeps a constant value. This is consistent with the phenomenon, as shown in Fig. 5, that the integrated current value becomes constant (the tail gets shorter while the pulse height gets higher), when the applied voltage is +40 V or more.

ISBN: 978-3-95450-201-1 doi:10.18429/JACoW-IBIC2018-TUOB03

Proportionarity of the Pulse Height

In order to evaluate the response (linearity) of the pulse height to the incident X-ray, the pulse height of the pulse train part of the filling pattern "1/7 filling + 5 bunches" is compared with the bunch current of the storage ring, as shown in Fig. 7. The bunch current in the vertical axis (right) is scaled to match the pulse height of the leadoff pulse (Fig. 7 (a)). It can be seen that the pulse height is proportional to the bunch current of the storage ring. However, the second and subsequent pulses are about 10% higher than the bunch current. The reason for this is that pulses are piled up on the tail of the preceding pulses even in the middle part of the train, just as the tail is seen in the last pulse of the pulse train (Fig. 7 (b)).

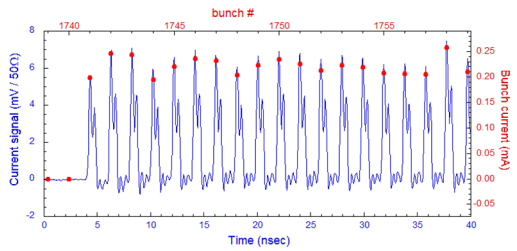

(a) Head of pulse train

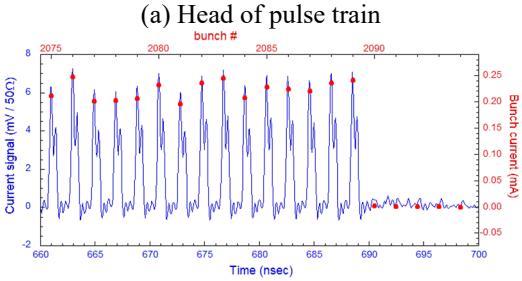

(b) Tail of pulse train

Figure 7: Pulse waveform (blue line) vs bunch current (red dot).

Generation of Position Sensitive Signal

In order to convert current signals to position information, it is necessary to quantify the charge of each pulse. We confirmed that it is possible to generate directly the position sensitive signal by combing the raw current signal of the pulse rather than individually quantizing the raw current signals. Figure 8 shows the setup of generation of position sensitive signal. The UR (Upper-Right) signal is split into two by a divider, one is connected to the oscilloscope and the other is reversed in phase at the short end of the tip of the stub cable. The LR (Lower-Right) signal is kept at the same phase by setting the tip of the stub cable to the open end. A “difference” signal is generated by combining the inverted UR signal and the strait LR signal. Figure 9 shows the experimental results. The preceding pulse is a "sum" signal in which each of the UR signal and the LR signal is combined via the shortest path. The pulse after about 8.6 ns is the "difference" signal combined after being reflected at the tip of each stub cable. The charge of the pulse of the "sum" signal is constant even when the monitor is scanned by 0.1 mm step in the vertical direction. On the other hand, the pulse height of the "difference" signal responds sensitively to the beam position.

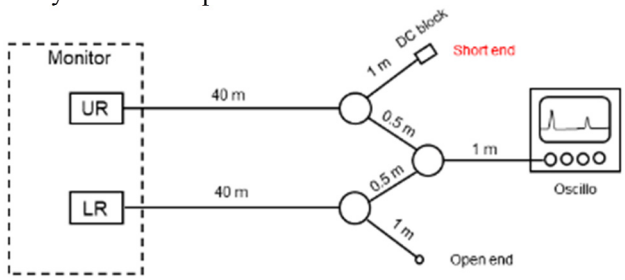

Figure 8: Setup of generation of position sensitive signal.

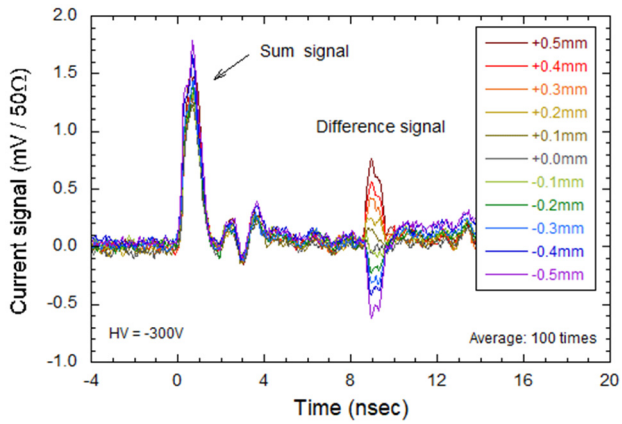

Figure 9: Observed position sensitive signals.

PERFORMANCE IN DC MODE

Position Sensitivity and Resolution

Although this monitor is optimized for pulse mode measurement, it can be used in the same way as conventional XBPMs. To evaluate the position sensitivity of this monitor, vertical scan measurements were performed. Figure 10 shows the results of the scan measurement in steps of 0.2 mm. A value of 1.25 was obtained as the correction coefficient Ay. In addition, it can be seen that the linearity is maintained over a wide range of the vertical scanning range (vertical position = ± 0.5 mm). Figure 11 shows the results of scan measurement in steps of 1 μm at 1 minute interval to evaluate the resolution. Each data was acquired with samplings every 6 seconds using an ADC with a time constant of about 1 s. From this result, the resolution of 0.12 μm RMS was obtained.

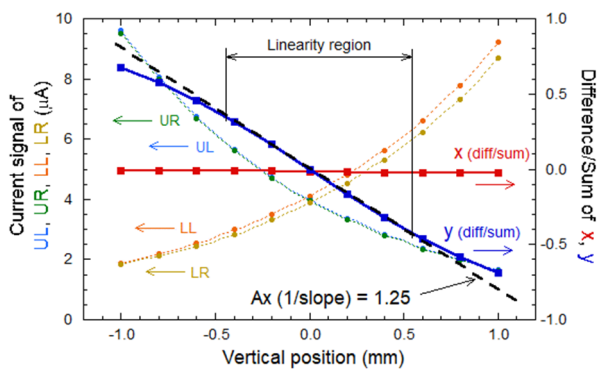

Figure 10: Scan measurement in 0.2 mm step.

ISBN: 978-3-95450-201-1 doi:10.18429/JACoW-IBIC2018-TUOB03

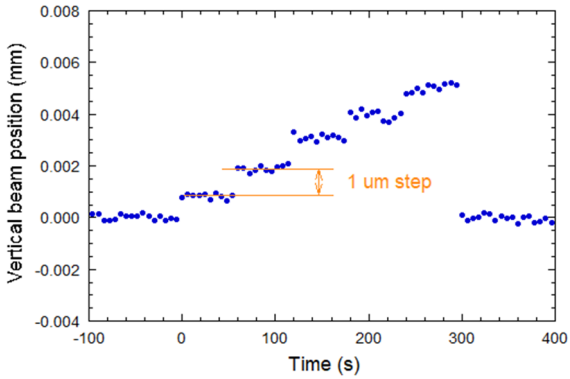

Figure 11: Scan measurement in 1 μm step.

Proportionarity of Current Signal

As shown in Fig. 12 (a), the sum signal of the four blades is proportional to the ring current of the storage ring. The result of calculation of "difference/sum" of the four blades is shown in Fig. 12 (b). For the vertical direction (y), as the ring current increases, the displacement of about 4 μm is observed significantly. On the other hand, no movement in the horizontal direction (x) has been observed because the radiation from the bending magnet beamline spreads in the horizontal direction. This indicates that this monitor operates normally even in the DC mode when the ring current is 10 mA or more.

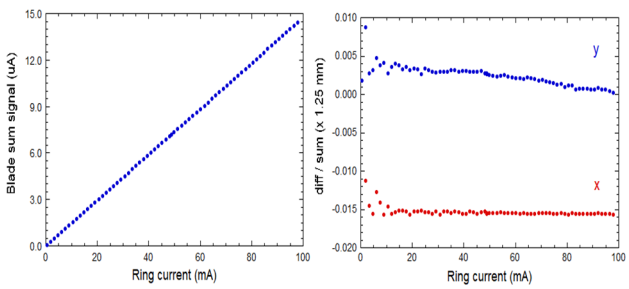

(a) (b)

Figure 12: Proportionarity in DC mode. (a) Blade sum signal vs ring current. (b) Difference/Sum vs ring current.

Long-term Stability

This monitor can be regarded as having a pair of left and right XBPMs for vertical measurement of the same type equipped with two upper and lower blades. In principle, the calculated vertical positions should have the same behaviour in both the left and right XBPMs. Figure 13 shows a trend graph over two months of the vertical position from the left and right XBPMs and the difference of them. Each data was acquired with samplings every 6 seconds using an ADC with a time constant of about 1 s. The value of the difference drifted by about 0.2 μm after short shut down of several days. In addition, the difference over the whole period of 0.14 μm RMS was observed, which corresponds to the resolution of the XBPM. The stability is demonstrated to be very good for two months.

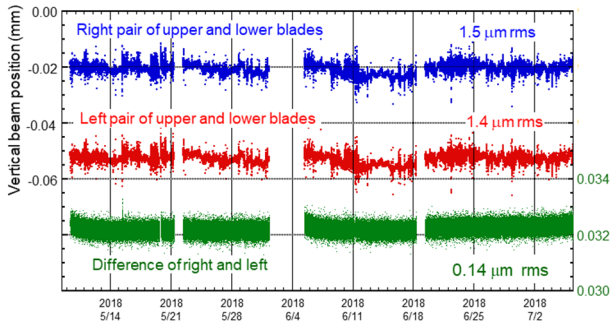

Figure 13: Stability in three months.

CONCLUSION

The pulse-by-pulse XBPM has been newly designed and manufactured, and performance tests were carried out at the SPring-8 bending magnet beamline BL02B1 front end. A unipolar single pulse of 0.8 ns FWHM was obtained. We qualitatively understood the cause of the double peak of the pulse. The pulse height is proportional to the bunch current of the storage ring and the pulse waveform can be controlled by adjusting the voltage of the collector. We demonstrated that the position sensitive signal can be generated directly by combining reflected pulses at the open end and the short end of the stub cables. In the DC mode operation, the correction coefficient Ay of 1.25 was calculated from the vertical scan measurements and the resolution of 0.12 μm RMS was obtained. In addition, good long-term stability was confirmed.

ACKNOWLEDGEMENTS

The authors would like to thank T. Nakamura, K. Kobayashi, S. Kimura and H. Osawa of Japan Synchrotron Radiation Research Institute (JASRI) for the useful advice regarding high frequency analysis. The design and fabrication of the pulse-by-pulse XBPM has been achieved by getting cooperation of Vacuum and Optical Instruments (Shinku-Kogaku, Inc., Tokyo, Japan).

REFERENCES

[1] H. Aoyagi *et al.*, *Nucl. Instr. and Meth. A*, Vol. 467-468, pp. 252-255, 2001.

[2] H. Aoyagi *et al.*, in *Proc. of the 12th Annual Meeting of PASJ,* 2015, pp.1224-1226.

[3] H. Aoyagi *et al.*, in *Proc. of the 3rd Annual Meeting of PASJ*, 2016, pp.159-162.

[4] H. Aoyagi *et al.*, in *AIP Conf. Proc. 879*, 2017, p1018.

[5] H. Aoyagi *et al.*, in *Proc. of DIPAC'11*, 2011, paper MOPD91, pp. 260-262.

[6] H. Aoyagi *et al.*, *Phys. Rev. ST Accel. Beams,* Vol. 16, p.032802, 2013.

[7] H. Aoyagi *et al.*, in *Proc. of the 13th Annual Meeting of PASJ,* pp. 1118-1121, 2016.

[8] H. Aoyagi *et al.*, in *Proc. of MEDSI'16*, paper WEPE10, pp.333-335.

[9] H. Aoyagi *et al.*, in *Proc. of the 14th Annual Meeting of PASJ*, 2017, pp.192-196.